Diverse K^+ Channels in Primary Human T Lymphocytes

SHERWIN C. LEE, DANIEL I. LEVY, and CAROL DEUTSCH

From the Department of Physiology, University of Pennsylvania, Philadelphia, Pennsylvania 19104-6085

ABSTRACT We used patch clamp techniques to identify and characterize a variety of K^+ channels in primary human peripheral T lymphocytes. The most common channel observed in cell-attached configuration was voltage gated and inactivating. In ensemble averages, the kinetics of its activation and inactivation were similar to those of the whole-cell, voltage-gated K^+ current described previously (Cahalan, M. D., K. G. Chandy, T. E. DeCoursey, and S. Gupta. 1985. *J. Physiol. [Lond.]*. 358:197–237; Deutsch, C., D. Krause, and S. C. Lee. 1986. *J. Physiol. [Lond.]*. 372:405–423), suggesting that this channel underlies the major portion of the outward current in lymphocytes. A small fraction of the time, this or another very similar channel was observed to inactivate significantly more slowly. Another channel type observed in cell-attached recording was seen less frequently and was transient in its appearance. This channel has a unitary conductance of ~10 pS, similar to the voltage-gated channel, but its voltage-independent gating, lack of inactivation, and different kinetic parameters showed it to be distinct. In whole-cell recording there is often a significant plateau current during sustained depolarization. Experiments using whole-cell and excised outside-out configurations indicate that at least part of this residual current is carried by K^+ and, as opposed to the predominant voltage-gated current, is charybdotoxin insensitive. These findings are consistent with evidence that implicates charybdotoxin-sensitive and -insensitive components in T lymphocyte proliferation and volume regulation.

INTRODUCTION

Circulating primary human T lymphocytes initiate and direct the specific response of the immune system to antigenic challenge. This response includes clonal expansion of antigenically restricted T cell populations and the elaboration of growth factors that control the growth and function of both T cells and antibody-producing B lymphocytes. The molecular mechanisms underlying these processes include control of ion movements. In the past few years new techniques have greatly expanded our understanding of lymphocyte physiology and biophysics (for review, see Grinstein

Address reprint requests to Dr. Carol Deutsch, Department of Physiology, University of Pennsylvania, 37th Street and Hamilton Walk, Philadelphia, PA 19104-6085.

Dr. Lee's present address is Department of Animal Physiology, University of California, Davis, CA 95616.

J. GEN. PHYSIOL. © The Rockefeller University Press · 0022-1295/92/05/0771/23 $2.00
Volume 99 May 1992 771–793

and Dixon, 1989). In particular, the application of patch clamp methods to cells of the immune system has revealed a variety of ionic conductances (for review, see Gallin, 1991). Subsequent studies have explored and confirmed the role of ionic conductances in immune cell functions (for review, see Grinstein and Dixon, 1989; Price et al., 1989; Lewis and Cahalan, 1990; Gallin, 1991).

The most prominent and best characterized conductance in human T lymphocytes is conferred by a voltage-gated K^+ channel (DeCoursey et al., 1984; Matteson and Deutsch, 1984; Cahalan et al., 1985; Deutsch et al., 1986, 1991). This K^+ conductance has been shown to contribute to the membrane potential of human T cells (Grinstein and Smith, 1990) and to be the major cation pathway in volume regulation of these cells subsequent to hypotonic shock (Deutsch and Lee, 1988; Lee et al., 1988; Grinstein and Smith, 1990). It has also been demonstrated that pharmacological block of this K^+ conductance inhibits mitogen-stimulated proliferation of T cells (Chandy et al., 1984; Deutsch et al., 1986; Price et al., 1989), at least in part because of effects on gene expression and elaboration of the autocrine growth factor, interleukin 2 (Price et al., 1989; Freedman et al., 1991).

Important issues remain concerning K^+ movement in T lymphocytes and the role of K^+ channels in cell function. First, although the whole-cell, voltage-gated K^+ current is well described, relatively little is known about this current at the single-channel level. Second, the mechanism by which the voltage-gated K^+ conductance supports cell proliferation is still unclear. Third, charybdotoxin (ChTX), a potent and specific blocker of the voltage-gated K^+ conductance (Price et al., 1989; Sands et al., 1989) does not inhibit stimulated T cell proliferation and interleukin 2 secretion as effectively as the less specific K^+ channel blockers (Price et al., 1989; Freedman et al., 1991), suggesting that other K^+ pathways may have a role in these processes. Among the possibilities are a Ca^{2+}-activated K^+ conductance that has been difficult to demonstrate directly in T cells (Tsien et al., 1982; Wilson and Chused, 1985; Grinstein and Smith, 1990; Grissmer and Cahalan, 1991), and a different, ChTX-insensitive K^+ efflux pathway that participates in volume regulation (Grinstein and Smith, 1990).

To address these questions the present work aimed to identify and characterize the voltage-gated K^+ channel and to search for other K^+-carrying channel types in normal human T lymphocytes. Using high-gain patch and whole-cell recording techniques, we acquired evidence for three distinct types of outward unitary K^+ current.

A preliminary account of this work has been presented (Lee et al., 1991).

MATERIALS AND METHODS

Cell Preparation and Culture

Blood was drawn from healthy adult human donors and peripheral blood mononuclear cells (PBMC) were isolated on a discontinuous Ficoll-Hypaque gradient as described previously (Deutsch et al., 1986). In some cases, the leukocyte byproduct of plateletpheresis was obtained from the Philadelphia Red Cross and PBMC were isolated in essentially the same manner.

When needed, bulk populations of purified T lymphocytes were produced by E-rosetting of PBMC with neuraminidase-treated sheep red blood cells (Deutsch et al., 1991).

PBMC were cultured in minimal essential medium supplemented with 10% human AB serum, nonessential amino acids, 2 mM glutamine, 100 μg/ml streptomycin, and 100 U/ml penicillin. Cells were incubated in siliconized glass tubes at 0.5×10^6/ml in a 5% CO_2 incubator at 37°C. Quiescent cells were maintained in culture and used for electrophysiological experiments for up to 3 d after isolation with no change in cell morphology or observed ion currents.

Preparation of Cells for Electrophysiology

PBMC were removed from culture and T lymphocytes were selectively adhered to bacterial grade 35-mm plastic Petri dishes (Falcon 1008, Becton Dickinson, Lincoln Park, NJ; or Corning 25050, Corning Glass Inc., Corning, NY) by the antibody procedure described previously (Matteson and Deutsch, 1984; Deutsch et al., 1986). Briefly, PBMC were incubated with a murine monoclonal antibody (Anti-Leu-5b; Becton Dickinson Immunocytometry Systems, Mountain View, CA) specific to the CD2 surface marker found on all human peripheral blood T lymphocytes. These cells were then selectively adhered to a plastic dish that had been preadsorbed with a goat antibody directed against murine IgG (product 4150; Tago, Inc., Burlingame, CA).

At other times, we wanted to prevent cell attachment to the dish. To generate such "floaters," we pretreated the dish with phosphate-buffered saline containing 5% fetal bovine serum. Conversely, to attach cells more tightly than the antibody-mediated procedure usually accomplished, we permitted cells to settle onto a clean tissue culture grade plastic Petri dish (Corning 25000; Corning Glass Inc.) in the absence of protein. All healthy lymphocytes will attach to the surface under these conditions. The method of attachment used in these studies did not affect the properties of the K^+ currents.

Electrophysiology

Standard patch clamp methods were used (Hamill et al., 1981; Deutsch et al., 1986). In all cases data were acquired with a List EPC-7 patch clamp amplifier (List Electronic, Darmstadt, Germany) controlled by a custom hardware/software system running on a PDP-11 computer (Digital Equipment Corp, Marlboro, MA). Some of the time the EPC-7 output was also sent to a digitizing VCR tape system based on a Sony PCM-501ES digital audio processor (after Bezanilla, 1985). Where needed, data were then recovered from the tape and analyzed off-line on the PDP-11 or on a 386SX-based PC using pCLAMP software (versions 5.5 or 5.5.1; Axon Instruments, Inc., Foster City, CA). Data were low-pass filtered with the 3-pole, 3-kHz Bessel filter in the EPC-7 or with an 8-pole Bessel filter with adjustable cutoff frequency (902LPF; Frequency Devices Inc., Haverhill, MA). All data are presented with the convention that positive outward current with respect to the cell is an upward deflection.

Three different patch clamp variations were used in these experiments: cell-attached, whole-cell, and excised outside-out. Since the lymphocyte membrane potential is primarily a K^+ diffusion potential (Deutsch et al., 1979; Wilson and Chused, 1985), all cells studied in the cell-attached mode were bathed in 140 mM extracellular K^+ solution to clamp the cell membrane potential to ~0 mV. The trans-patch potential gradient in cell-attached configuration would then be dependent solely on the potential applied to the pipette. This was generally true (however, see Fig. 5 in Results).

The high K^+ bathing solution contained (mM): 140 KCl, 10 NaCl, 2.5 $CaCl_2$, 1.0 $MgCl_2$, 5.5 glucose, 10 HEPES, and NaOH to pH 7.30 at 295–305 mosM. The pipette solution for cell-attached recording contained standard Ringer's solution in order to maintain the normal trans-membrane K^+ gradient across the patch. The Ringer's solution contained (mM): 140

NaCl, 5 KCl, 2.5 $CaCl_2$, 1.0 $MgCl_2$, 5.5 glucose, 10 HEPES, and NaOH to pH 7.30 at 295–305 mosM. Leak and uncompensated capacitive currents were digitally subtracted using appropriate trials in which no channels opened.

Cell-attached recordings were made with both a high–melting point borosilicate (34500; Kimble Glass Inc., Vineland, NJ) and a low–melting point lead glass (Corning 0010; Garner Glass Co., Claremont, CA). Pipettes were formed using a standard double-pull, and coated with Sylgard 184 (Dow Corning, Midland, MI) or Sigmacote (Sigma Chemical Co., St. Louis, MO; after Mahaut-Smith and Schlichter, 1989). Borosilicate pipettes were always fire-polished before use; with 0010 glass, fire-polishing was not required to form gigaohm seals. Electrical resistance with Ringer's in the pipette was typically 4–5 MΩ for both glasses.

The best glass we found for cell-attached recording was the Corning 0010. With both glasses, high-resistance seals were readily obtained, but we saw channels more consistently with the 0010 glass. Channel properties as obtained with both glasses in cell-attached configuration were identical. Typical apparent seal resistance for the borosilicate glass was 20–100 GΩ, while seal resistance with 0010 glass was usually 50–200 GΩ.

We considered that the membrane could be subjected to stress if there were manipulator drift during long-term, cell-attached recording from adhered cells. To allay this concern, some experiments were done using floaters, E-rosetted cells discouraged from attachment by the procedure described above.

Whole-cell recordings were done as described previously using pipettes of borosilicate glass coated with Sylgard (Deutsch et al., 1986; Deutsch and Lee, 1989; Lee and Deutsch, 1990). Linear leak and capacitive currents were subtracted by the procedure of Armstrong and Bezanilla (1974) as described (Deutsch et al., 1986). All whole-cell experiments were done using antibody-selected and -adhered T lymphocytes maintained in a normal Ringer's bath solution. The pipette solution contained (mM): 130 KF, 11 K_2EGTA, 1 $CaCl_2$, 2 $MgCl_2$, 10 HEPES, and KOH to pH 7.2 at 275–295 mosM.

Excised outside-out patches were pulled from cells soon after entering whole-cell configuration. The solutions and pipettes used for excised patches were the same as for whole-cell recording. Leak and capacitive current were subtracted using appropriate records in which no channels opened.

All experiments were performed at room temperature (20–25°C).

Reagents

ChTX was obtained from M. Garcia (Merck, Sharp & Dohme, Rahway, NJ) as a purified toxin from scorpion venom and was made up as a stock solution at 10 μM with 0.2% (wt/vol) bovine serum albumin, or from C. Miller (Brandeis University, Waltham, MA) as a recombinant protein and made up at 18 μM in 15 mM sodium phosphate; EGTA, HEPES, and bovine serum albumin were obtained from Sigma Chemical Co.; tetraethylammonium chloride (TEA) was from Eastman Kodak Co. (Rochester, NY) and was recrystallized before use. All salts were reagent grade.

RESULTS

Several types of unitary events were observed in human peripheral blood T lymphocytes using the cell-attached patch clamp configuration.

Voltage-gated Channel

The most prevalent type of unitary event was an outward current that gated with membrane depolarization. Patches exhibiting this type of behavior contained an

average of 1.7 ± 0.9 (SD; n = 70; range 1–4) such channels, but there were many patches with no activity. Threshold for activation of current was approximately −45 mV, as shown in Fig. 1 *A*. Successively larger depolarizations showed increased current amplitude and decreased latency to opening.

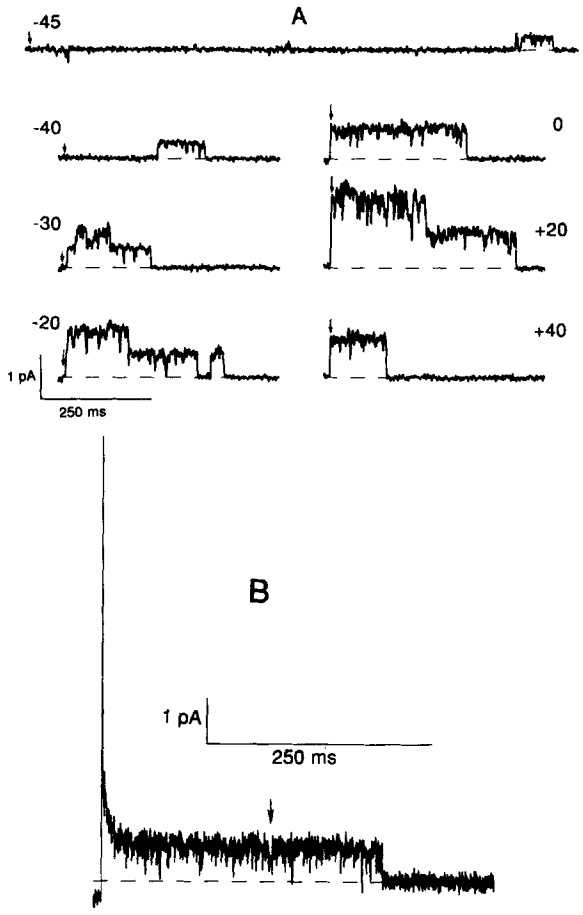

FIGURE 1. Voltage-gated single-channel currents observed in cell-attached patch recording. (*A*) Representative currents at the membrane potentials indicated from a single patch. This cell was a PBMC "floater." Holding potential for the patch was −90 mV. Voltage steps began at times indicated by arrows and were applied for 5 s. Except for the example at −45 mV, for which activity continued beyond the period shown, none of the other examples in this figure exhibited activity beyond the 0.5 s presented. These data were acquired with a sampling rate of 2 kHz and low-pass filtered at 250 Hz. (*B*) A representative record of a single-channel current less stringently filtered. These are exactly the same data as the 0-mV record in *A* at 10-kHz sampling and 1-kHz filter. Leak and capacitive currents were *not* subtracted from this record. The difference between the holding current before the step (*far left*) and that at 0 mV after the channel has closed (*far right*) indicates a seal resistance of ~250 GΩ. Periods of approximately half-unitary current amplitude (*arrow*) were infrequently observed.

The unitary conductance for the patch in Fig. 1 was 8.6 pS, obtained from a linear regression of the current versus voltage plot (Fig. 2). This value is similar to previous estimates from electrophysiological studies (Cahalan et al., 1985; Deutsch and Lee, 1989; Lee and Deutsch, 1990). The extrapolated reversal potential was −83.9 mV, consistent with a highly selective K^+ channel and a calculated K^+ Nernst potential of

−87 mV. The average of three such analyses yielded a unitary conductance of 9.4 ± 1.2 pS and an extrapolated reversal potential of −84.0 ± 5.4 mV. At voltages greater than 0 mV, the current amplitude was no longer linear with voltage.

Generally, channels opened and exhibited prolonged bursting behavior during the first few hundred milliseconds after depolarization. After the burst period, channels closed and rarely reopened during 5 s of maintained depolarization in the range −20 to +50 mV. When the patch was returned to the holding potential, recovery from this inactivated state required many seconds. Although we did not quantify this recovery period, we utilized closely spaced depolarizations to explicitly generate blank records that were used to subtract leak and capacitive current. At voltages near threshold (approximately −45 to −40 mV), channels reopened intermittently throughout the 5-s voltage step, consistent with slower entry into the inactivated state. However, channels in patches held for extended periods at any voltage positive to the threshold became inactivated.

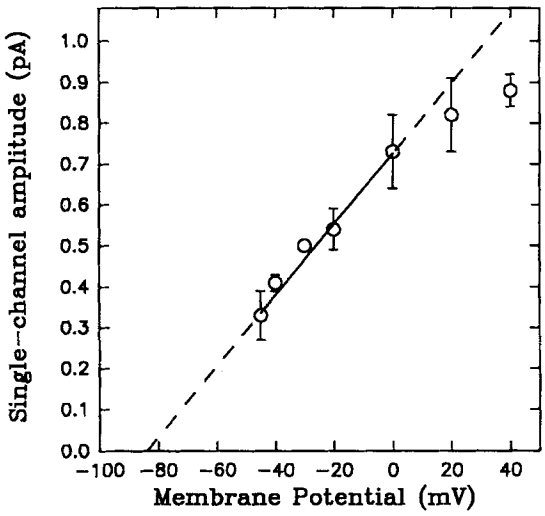

FIGURE 2. Single-channel current–voltage relation for the voltage-gated channel from the same patch as Fig. 1. Determination of single-channel amplitude was restricted to periods in which only one channel was open. A linear regression fit of channel amplitude between −45 and 0 mV (*solid line*) gave an extrapolated reversal potential (*dashed line*) of −83.9 mV and a unitary conductance of 8.6 ± 0.5 pS. Error bars represent standard deviations.

To characterize the mean open and closed times of this channel, we used the standard 50% amplitude criterion to assign open and closed events for the patch in Fig. 1. Table I gives the open and closed state dwell times as a function of voltage. As shown in Fig. 1 *B*, some of the larger downward deflections observed at 250 Hz filtering do in fact go completely to baseline and represent brief channel closure when observed at wider bandwidth. Both open and closed histograms were well fit with single exponentials: mean open time was ~ 10 ms and mean closed time was ~ 1 ms. In all-points amplitude histograms (not shown) there was a monotonic increase in the variance of the open-channel distributions with increasing depolarization.

We determined the burst length of open-channel activity as a function of voltage by measuring the time between first opening and final closing for records in which only a single channel opened. Histograms were generated from these data and each was fit with a single exponential (data not shown). The time constants for these fits are given under "Open 2" in Table II.

TABLE I

Dwell Times for Voltage-gated Channel

V	Open	Closed 1
mV	*ms*	*ms*
−20	7.4	0.93
0	10.9	0.99
+20	11.4	0.73

Data for these analyses were acquired from VCR tape recordings of the same patch as Fig. 1, using a 10-kHz sampling rate and a 1-kHz filter. Dwell times were determined with pCLAMP software (Axon Instruments, Inc.). Extended periods in which one channel was active were the only data used to analyze open and closed dwell times. Because this channel inactivates, it is unlikely that periods showing the activity of a single channel were contaminated with activity of the second channel.

The latency to first opening of this voltage-gated channel was highly dependent on membrane potential (Table II). Cumulative distributions of first latencies as a function of voltage for the patch in Fig. 1 are shown in Fig. 3. These data have been normalized to a probability of 1.0 and corrected for a patch containing two channels (Patlak and Horn, 1982). First opening can occur quite late after the voltage step at −20 mV (median first latency 10 ms), and this delay decreases at +20 mV (median first latency 3 ms). A similar delay in the activation of macroscopic T cell K^+ current has been noted before (Cahalan et al., 1985; Lee and Deutsch, 1990).

TABLE II

Average Kinetic Parameters for Voltage-gated Channel

	Single channels		Ensemble*		
V	Median‡ latency	Open 2§	Act	Half-rise‖	Inact¶
mV	*ms*	*ms*	*ms*	*ms*	*ms*
−20	10.0	120.3	4.9	9.0	120
0	7.0	122.0	2.5	4.6	120
+20	4.0	58.7	2.15	4.0	60 225, 0.15
+40	3.0	103.9	1.5	2.8	95 420, 0.15

*The number of pulses per summed ensemble at each voltage was 12, 13, 9, and 6 for −20, 0, +20, and +40 mV, respectively. Data were fit with a model of the form

$$I = k[1 - \exp(-t/\tau_a)]^4 \exp(-t/\tau_i)$$

where I is current, t is time, k is an arbitrary scaling factor, and τ_a and τ_i are the activation and inactivation time constants, respectively.

‡Median latency was determined from normalized cumulative distributions of first latencies shown in Fig. 3.

§Best-fit single exponential to distribution of burst length; only records with a single open channel were used for this determination.

‖Half-rise time for n^4 model is 1.838 times τ_a.

¶Best-fit single or double exponential to falling phase of ensemble current; where two components gave a better fit, the last number of the triplet is the fraction of the total associated with the longer time constant.

Normalizing the opening probability to 1.0 excludes consideration of channels that did not open. In most patches we studied, the maximum number of channels we observed in the patch would open with every strong depolarization; when consistently fewer than the maximum number of channels opened, it usually signified the imminent or actual permanent loss of a channel.

To deduce the macroscopic properties of this channel, we constructed ensembles of the single-channel currents obtained from the patch shown in Fig. 1. These results are shown in Fig. 4 with the calculated best-fit time constants superimposed, assuming a fourth power exponential for activation and a single or double exponential function for inactivation, as described previously (Cahalan et al., 1985; Lee and Deutsch, 1990). Table II compares the major kinetic parameters derived from first

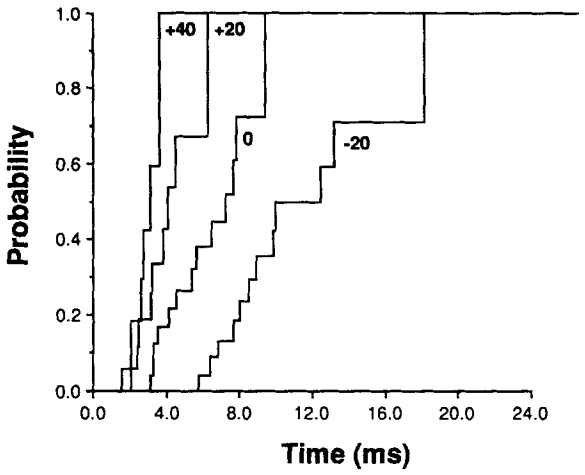

FIGURE 3. Voltage dependence of latency to first opening for the voltage-gated channel. The same data set used for Figs. 1 and 2 was analyzed on the PDP-11 at 10-kHz sampling rate and 1-kHz filter. The time between imposition of the voltage step and channel opening was determined manually from the computer display. The first latency distribution function for one channel in a patch, F_1, was calculated from the first latency distribution function for two channels in a patch, F_2, by the equation $F_1 = 1 - (1 - F_2)^{1/2}$. This figure presents the probability (F_1) that at least one channel has opened by the times indicated. Cumulative distributions of first latencies are normalized to a probability of 1.0.

latency and open-channel dwell time analyses with the activation and inactivation time constants, respectively, derived from the single-channel ensembles. There is reasonable agreement between the time constants that characterize the open-channel burst length (Open 2) and ensemble/macroscopic inactivation, suggesting that burst length determines the rate of macroscopic inactivation. This correlation is possible only because the first latency is brief compared with the inactivation time constant. However, this comparison should be viewed with the caveat that the data may be biased by selection of periods in which only a single channel was active. Both the median latency and the calculated half-rise time of the ensemble current decreased with increasing depolarization.

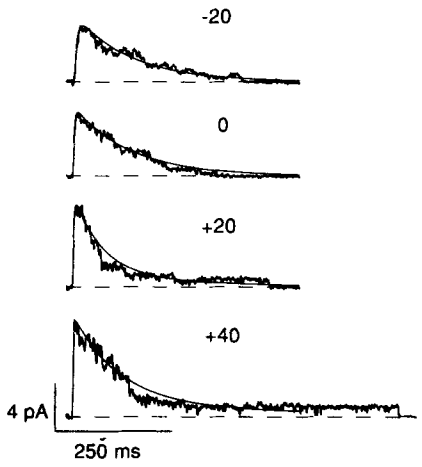

FIGURE 4. Ensemble currents for the voltage-gated channel. Voltage-gated single-channel currents as shown in Fig. 1 *A* (250-Hz filter, leak and capacitive current subtracted) were added together and then scaled to an equal number of trials. The ensemble data were fit with a Hodgkin-Huxley equation to generate activation and inactivation time constants as a function of voltage (Table II).

A better description of inactivation at positive membrane potentials was sometimes afforded by the inclusion of a second exponential term. This term described a minor current which decayed more slowly than the major current. The minor current comprised 10–30% of the total current. However, in 4 patches out of 70 that showed voltage-gated currents, bursts of activity lasting a second or more were the predominant single-channel activity observed, and this slower component inactivated with a time constant approximately four times longer than normal (data not shown). Except for slower inactivation, these current records were not distinguishable from other voltage-gated currents.

Table III summarizes the activation and best-fit single exponential inactivation time constants from five ensemble current sets obtained from five different cells. All of these data were of the most common, fast-inactivating type. When compared with the corresponding values for activation and inactivation of the macroscopic current,

TABLE III

Time Constants for Activation and Inactivation

Ensemble*			Whole Cell‡					
			Act			Inact		
V	Act	Inact						
mV	*ms*	*ms*		*ms*			*ms*	
−20	6.6 ± 3.7	150 ± 46	19.5	37.5	10.0	320	421	360
0	3.7 ± 2.3	132 ± 28	7.7	15.7	3.6	188	315	190
+20	2.6 ± 0.9	134 ± 38	5.3	10.1	1.9	188	253	190
			Ref. 1	Ref. 2	Ref. 3	Ref. 1	Ref. 2	Ref. 3

Data were fit with a Hodgkin-Huxley (1952) type n^4j model as described for Table II.

*Average of five data sets of single-channel ensembles obtained from five different cells.

‡Literature whole-cell time constants, where Ref. 1: representative cell with 140 mM F^- pipette solution; Cahalan et al., 1985; Ref. 2: average of seven cells with 40 mM F^- pipette solution; activation time constants were converted to the fourth power formulation; Deutsch et al., 1986; Ref. 3: representative cell with 130 mM F^- pipette solution; Lee and Deutsch, 1990.

these values have the same voltage dependence but are somewhat shorter than those obtained from whole-cell patch clamp studies (also included in Table III; Cahalan et al., 1985; Deutsch et al., 1986; Lee and Deutsch, 1990).

In summary, this K^+ channel opened upon membrane depolarization with a delay that was voltage dependent. Once open, especially as a result of strong depolarization, the channel remained open for an extended period, except as interrupted by intermittent brief closures of ~1 ms. When the channel closed for a period longer than 1 ms, it was then rare for it to reopen during 5 s of maintained depolarization. The length of this burst of activity before the onset of inactivation was not convincingly voltage dependent. Ensembles of this channel reproduce the voltage dependence and most of the characteristics of the voltage-gated macroscopic current, suggesting strongly that this channel underlies the majority of whole-cell current.

How Good Is Voltage Control?

We often observed changes of the single-channel amplitude during a step depolarization to a fixed pipette potential. An example of this phenomenon is shown in Fig. 5.

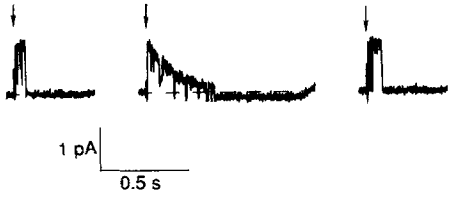

FIGURE 5. Change in unitary amplitude while the channel is open: variation of cell voltage in cell-attached patch configuration. Consecutive depolarizations to +30 mV from a holding potential of −90 mV were applied ~40 s apart. The voltage steps began at the times indicated by the arrows and were maintained throughout each of these traces. This cell was antibody selected and adhered. Measured apparent seal resistance was 150 GΩ. Sampling rate was 2 kHz and filter was 250 Hz.

Three consecutive depolarizations of this patch, which contained a single voltage-gated channel, demonstrate the variable nature of the effect. A decline in open-channel current, as illustrated in the middle trace, was observed periodically during recording in ~25% of all patches with channels; this behavior was even more common in recordings from cells in normal Ringer's and was almost universal in patches with three or four channels. Our interpretation of such behavior is that the opening of the channel(s) in the patch is sometimes sufficient to perturb the membrane potential of the whole cell, even in high K^+ bathing media. When the total cell conductance is relatively low, the opening of K^+ channels in the patch will tend to hyperpolarize the potential of the cell, changing the absolute potential across the patch and reducing the driving force for K^+ movement through the open channels in the patch.

For example, assuming 10 pS unitary conductance and a reversal potential of −83 mV (Fig. 2), the change in amplitude of the open channel in the middle trace of Fig. 5 is consistent with a shift of the whole-cell potential from 0 to approximately −60

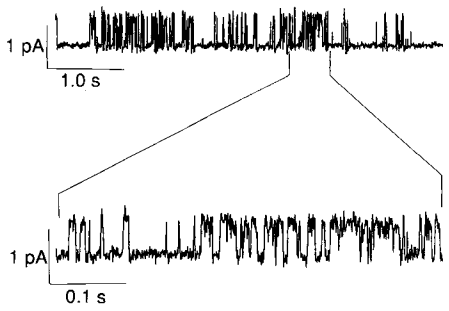

FIGURE 6. Continuous activity of a noninactivating outward current. This cell was a PBMC floater. The upper trace shows 5.12 s of single-channel activity in a patch held at 0 mV. The lower trace is a 10-fold expansion of the indicated period. The sampling rate was 5 kHz and the filter was 500 Hz.

mV. This change in whole-cell membrane potential was also reflected in the holding current after the channel closed. The rate at which the closed-channel holding current relaxed indicates that total cell resistance could be ≥ 100 GΩ, equivalent to one or zero open voltage-gated channels in the entire cell (analysis after Fenwick et al., 1982).

We should emphasize that in the construction of single-channel ensembles as in Fig. 4, we were very careful to exclude records displaying evidence of membrane potential instability as exhibited in Fig. 5.

Noninactivating Channel

A different type of single-channel behavior was observed in 15 of 80 patches with unitary activity. This channel did not inactivate and could be continuously active at all voltages. Fig. 6 shows 5.12 s out of almost 4 min of such activity observed in a patch held at 0 mV. This channel was characterized by both rapid flickering during open-channel bursts and intermittent silent periods. The voltage dependence of this conductance is shown in Fig. 7 for a voltage ramp from +20 to −70 mV. The reversal potential was negative to −80 mV, indicating that this channel is K^+ selective.

This channel type was usually active immediately or soon after seal formation, and rarely persisted more than a few minutes. It was observed together with voltage-gated, inactivating channels of the type described above, and by itself. The unitary conductance of the noninactivating channel was 8.2 ± 0.7 pS (n = 3) when analyzed in the range negative to 0 mV; single-channel magnitude was less than expected at

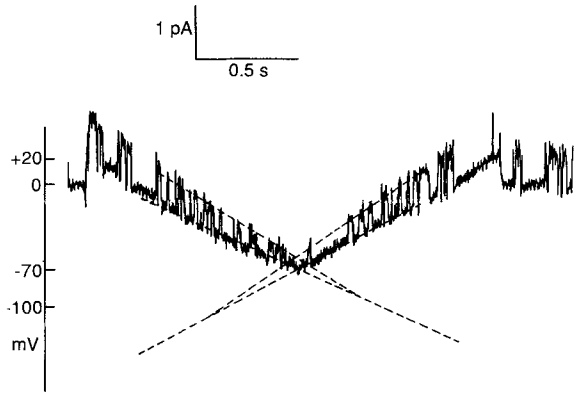

FIGURE 7. Noninactivating outward current during a voltage ramp. The patch of Fig. 6 was subjected to a 2.0-s voltage ramp from +20 to −70 mV and back to +20 mV. Holding potential remained 0 mV. Seal resistance was ~45 GΩ. Extrapolated reversal potential was approximately −100 mV. The low-pass filter was 100 Hz.

potentials >0 mV. This unitary conductance is not significantly different from that determined for the inactivating channel.

To further characterize this current, we analyzed the dwell times of the single-channel records. The open-channel dwell-time histogram for the complete data set of Fig. 6 (Fig. 8*A*) was fit with two exponentials to give time constants of 1.8 and 4.2 ms. The dwell time histogram for the closed state at 0 mV (Fig. 8 *B*) was fit with four time constants of 0.5, 4.9, 24, and 224 ms. The time constant of ~0.5 ms

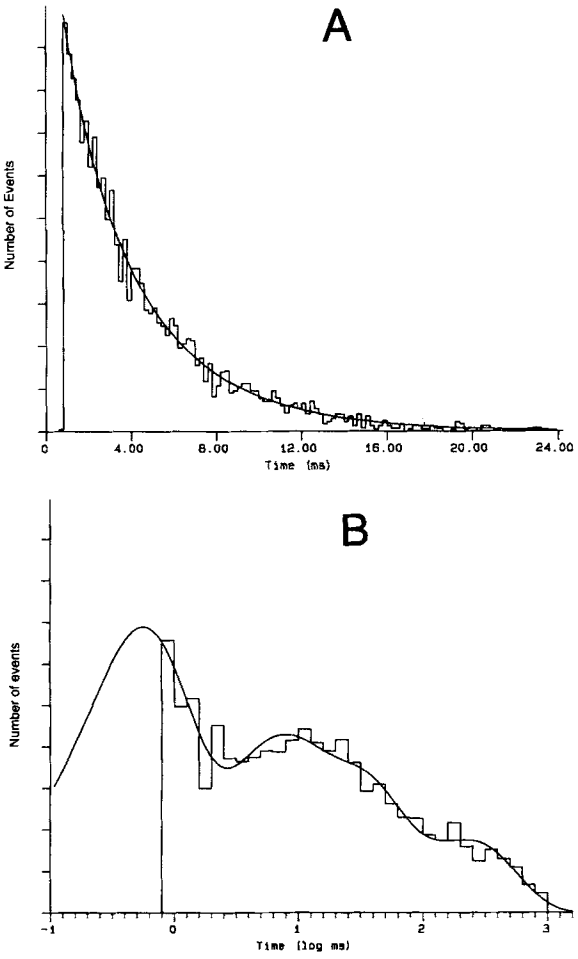

FIGURE 8. Dwell-time analysis of the noninactivating channel at 0 mV. The data of the patch of Figs. 6 and 7 were sampled at 5 kHz and filtered at 500 Hz. (*A*) Open-time histogram. The data were fit best with two time constants of 1.8 and 4.2 ms. There are 3,994 events in this histogram. (*B*) Closed-time histogram. This is a log-binned histogram with counts plotted as the square root. The data were fit best with four time constants of 0.50, 4.9, 24.3, and 224 ms. There are 3,184 events in this histogram.

characterizes the relaxation of baseline noise at this filtering and is unlikely to describe a true channel process. The averages for three such analyses are presented in Table IV. As was the case for the inactivating channels, there was no noticeable voltage dependence of either the open or closed times in the range of −20 to +20 mV, and there was a monotonic increase in amplitude variance with increasing depolarization as revealed in all-points amplitude histograms (data not shown). However, the kinetic parameters needed to describe the noninactivating channel are

more complex. The distinguishing feature of this channel is that it has closed-time components that are comparable to, or longer than, the mean open time, whereas excursions to the closed state for the voltage-gated channel are very brief until the onset of inactivation.

As the noninactivating channel appeared to be K^+ selective and usually active only immediately after seal formation, we hypothesized that this could be a Ca^{2+}-activated K^+ channel similar to that underlying the occasional transient activity during patch formation on human B lymphocytes and rat thymocytes reported by Mahaut-Smith and Schlichter (1989). However, we could neither activate nor sustain the activity of this channel in cell-attached patches on human T cells using bath-applied Ca^{2+} ionophores (A23187 and ionomycin, at concentrations up to 1 μM) under conditions expected to increase intracellular free Ca^{2+} (Fasolato and Pozzan, 1989; Mahaut-Smith and Schlichter, 1989; Grinstein and Smith, 1990). We were also unable to provoke or inhibit channel activity by positive or negative pressure.

TABLE IV

Dwell Times for Noninactivating Channel

	O1	O2	C1	C2	C3	C4*
Patch 1						
−20 mV		4.3	0.44	3.8	21.1	138
0 mV		4.4	0.48	5.0	31.9	265
+20 mV		3.8	0.43	3.3	8.2	79
Avg		4.2	0.45	4.1	20.4	161
(3)		±0.3	±0.03	±0.9	±11.9	±95
Patches 2 and 3						
0 mV	1.6	4.0	0.42	3.4	19.0	153
(2)	±0.2	±0.2	±0.12	±2.1	±7.5	±100
Avg All	1.6	4.1	0.43	3.8	19.9	158
(5)	±0.2	±0.3	±0.06	±1.3	±9.2	±84

These data were sampled at 5 kHz and filtered at 500 Hz for patches observed as described in Fig. 6. O and C are open and closed dwell times, respectively.

*The longest time constant was highly variable and dependent on which interval of data was used for analysis; we excluded occasional silent periods of more than a few seconds duration.

Charybdotoxin-insensitive Current in Whole-Cell Mode

Diversity of K^+ channels was also manifested in whole-cell mode. Typically, outward current elicited by strong depolarization includes the normal, inactivating current and a small component of noninactivating plateau current. During long-term, sustained depolarization, even the plateau current tends to diminish with time, leaving a residual amount of activity that is sometimes sufficiently quiet to be able to distinguish individual unitary events in whole-cell mode (Cahalan et al., 1985; Deutsch and Lee, 1989; Lee and Deutsch, 1990). Fig. 9 *B* is an example of such residual activity. Cahalan and co-workers (1985) interpreted residual channel activity

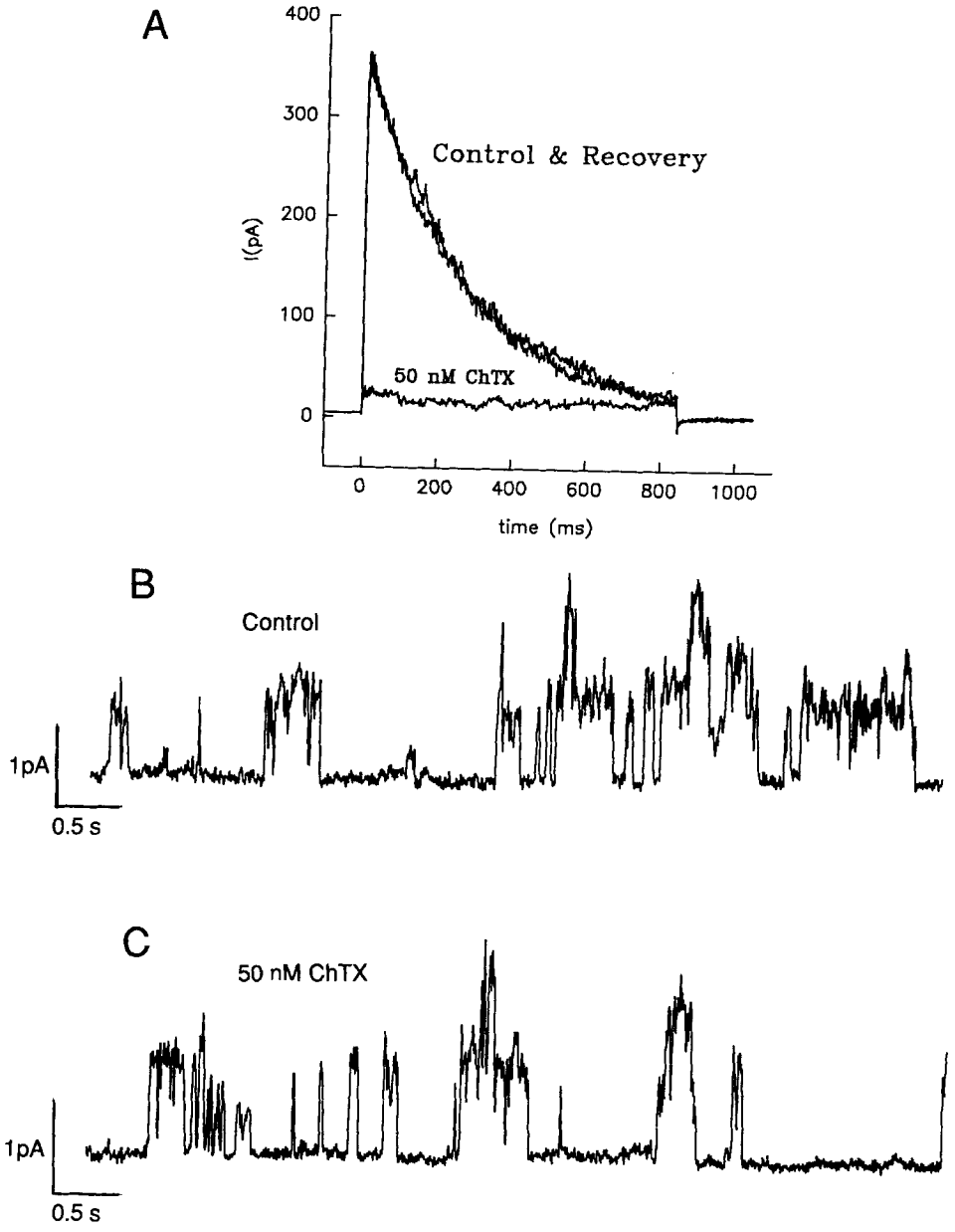

FIGURE 9. ChTX-sensitive and -insensitive whole-cell currents. This was an antibody-selected and -adhered cell. *A* shows whole-cell voltage-gated current in response to depolarization from −70 to +50 mV. The "control" trace was taken 67 min after entering whole-cell configuration. The cell was held at +30 mV for a few minutes, and then residual single-channel activity was recorded and a sample is shown in *B*. 8 min after the recording shown in *B*, a macropipette containing 50 nM ChTX in Ringer's solution plus 0.1% BSA was brought within 30 μm of the cell. After 1 min the trace shown in *C* was recorded. The cell was then repolarized to −70 mV and the macroscopic current elicited by a step from −70 mV to +50 mV was recorded (*A*, "50 nM ChTX"). The "recovery" trace was taken 6 min after ChTX was removed. All macroscopic current records were sampled at 20 kHz for the first 25.6 ms of the pulse and at 500 Hz for the remainder of the pulse and filtered at 3 kHz. All single-channel recordings in this experiment were 79 s in duration, sampled at 2 kHz, and filtered at 493 Hz.

as reactivation of previously inactivated voltage-gated channels. However, this has been difficult to prove, and the following experiments suggest otherwise.

To identify the components of the whole-cell current, we used ChTX, which inhibits the voltage-gated K^+ current of T lymphocytes with a K_i of ~1 nM (Price et al., 1989; Sands et al., 1989). As shown in Fig. 9, for a cell in whole-cell configuration, we obtained the macroscopic current for a voltage step to +50 mV (control curve, Fig. 9 *A*) and the single-channel currents remaining after prolonged depolarization to +30 mV (Fig. 9 *B*). When this cell was moved into the stream of a macropipette containing 50 nM ChTX, it still showed residual unitary events (Fig. 9 *C*). Upon repolarization in the continued presence of 50 nM ChTX, the transient, inactivating current was reduced by 93% from control (Fig. 9 *A*). Removal of ChTX resulted in full recovery of the voltage-gated macroscopic K^+ current ("Recovery" curve, Fig. 9 *A*).

The effect of ChTX, if any, can be inferred from the closed-time duration. The proportion of time that all channels were closed in the experiment shown in Fig. 9 was estimated from the areas under Gaussian-fitted all-points amplitude histograms (not shown). The amplitude histogram was predominantly bimodal, with a large closed-channel peak and a smaller distribution of open channels centered about 0.7 pA. The proportion of time that all channels were closed in the absence and presence of ChTX was 56 and 69%, respectively. Similar results were obtained for this cell held at 0 mV, and from dwell time analyses. The increase in the proportion of time that channels were closed in the presence of ChTX was reversible. The number of channels in this cell, calculated from the ratio of peak macroscopic current to single-channel current, 360 pA/1.3 pA per channel at +50 mV, was 276. If the single-channel currents form a homogeneous population underlying the macroscopic current, the steady-state probability of a single channel being open in the absence of ChTX was $[1 - (0.56)^{1/276}] = 0.002$. In the presence of ChTX the steady-state probability of a single channel being open would be $0.002 \times 0.067 = 0.00013$ if the steady-state currents are ChTX sensitive, and the steady-state probability of a single channel being closed would be $(1 - 0.00013) = 0.99987$. The probability that no channels would be open would be $(0.99987)^{276} = 0.96$, which is significantly larger than 0.69 obtained from analysis of the amplitude histograms of the experiment presented in Fig. 9 *C*. We therefore conclude that the observed residual single-channel activity in the presence of ChTX cannot be explained by unblock of channels during the time of our measurements, and that much of the single-channel activity was insensitive to ChTX.

Fig. 10 *A* displays the current–voltage relations for another cell in the presence of 10 nM ChTX. Maximum current amplitude (peak) and the current amplitude at the end of 1.4 s (plateau) were plotted separately. Both currents increased with depolarization, but each had a different threshold for activation and a different sensitivity to voltage. Threshold for activation of the peak current was approximately −40 mV, as reported previously for the voltage-gated, inactivating current (Cahalan et al., 1985; Deutsch et al., 1986), whereas activation of the plateau current was most prominent positive to 0 mV.

The residual plateau current varied considerably in magnitude from cell to cell, and especially from donor to donor, and it decreased with time in whole-cell configuration when using a pipette solution containing a high concentration of F^-. In

Fig. 10 *B*, the upper trace shows the current in response to a step to +50 mV in the presence of 10 nM ChTX. The middle trace, marked +50*, shows the current in response to the same protocol 23 min later. The peak current remained the same, but the plateau was smaller. The difference record, +50 minus +50* (bottom trace), suggests that either there is time-dependent conversion of the plateau current into an inactivating form, or that there is a slow-activating, noninactivating component that is labile in whole-cell mode. Similar results were obtained at other voltages.

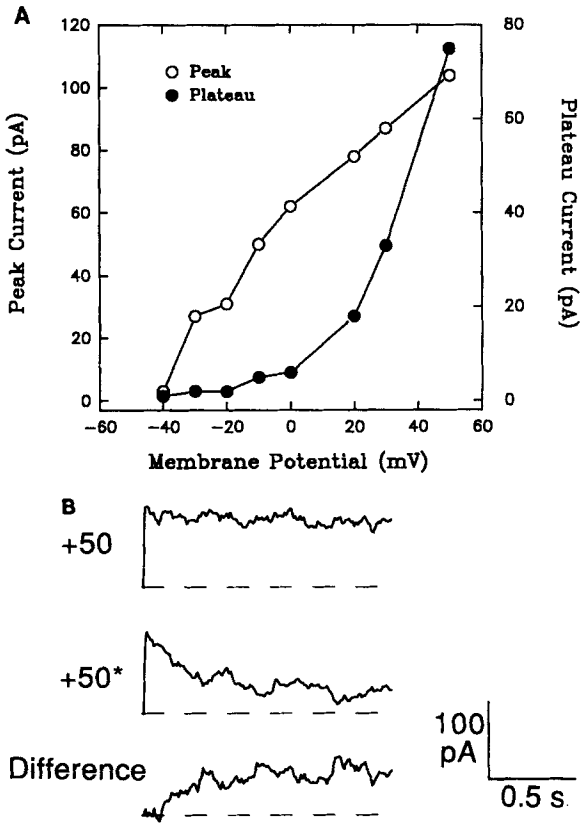

FIGURE 10. Voltage dependence of ChTX-insensitive current. An antibody-selected and -adhered T lymphocyte was placed into whole-cell configuration in the presence of 10 nM ChTX. (*A*) Current–voltage relation for ChTX-insensitive current. The cell was held at −70 mV and depolarized to a series of voltages in the period from 8.5 to 14.5 min after entering whole-cell configuration. This graph shows peak current and plateau current at 1.4 s as a function of voltage. Note different scales. (*B*) Decrease in plateau current as a function of time after entering whole-cell configuration. The upper trace is the current in response to a 1.4-s step from −70 to +50 mV in the presence of 10 nM ChTX (this is the +50-mV point in the graph in *A*). The middle trace is the current in response to the same voltage step 23 min later. The bottom trace is the difference of upper − middle. The sampling rate was 500 Hz, and the data were filtered at 2 kHz.

The small size of the residual plateau current made an unambiguous determination of its reversal potential difficult. Nevertheless, the residual outward current appears to be carried by K^+ based on experiments using intracellular blockers. When we used a pipette solution that contained 130 mM CsF in place of an equal amount of KF, a very small voltage-dependent, inactivating current remained at positive potentials, although significant inward "tail" current still occurred on repolarization (data not shown). However, no distinguishable unitary events of any kind could be seen at depolarized voltages, suggesting that the small remaining outward current

was the result of very low Cs^+ permeation. When the pipette solution contained 140 mM TEA-Cl in place of KF, no voltage-gated current of any sort, including tail currents, could be elicited, and no unitary events could be detected.

Further evidence for a ChTX-insensitive K^+ channel comes from experiments using excised patches. In the upper trace of Fig. 11, depolarization to 0 mV elicits the opening of two or three channels in an outside-out patch. After adding 19 nM ChTX to the bath (middle trace), only a late-opening channel was observed. When 10 mM TEA^+ was added in addition to the ChTX (bottom trace), the unitary amplitude of the late-opening channel was approximately halved. Reduction of single-channel amplitude by TEA is a signature of K^+ channels (e.g., DeCoursey et al., 1987). It is unlikely that this ChTX-insensitive K^+ channel is the human counterpart to the ChTX-insensitive "1 type" K^+ channel described in murine lymphocytes and thymo-

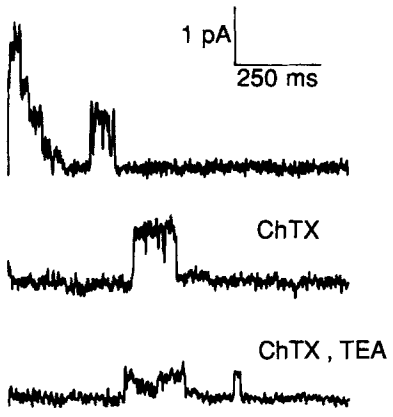

FIGURE 11. Effect of blockers on single-channel currents. PBMC were allowed to attach to a clean tissue culture grade plastic Petri dish in normal saline. A flattened cell was placed into whole-cell configuration, and the pipette was pulled away to yield an excised outside-out patch. This was held at −90 mV and depolarized to 0 mV to elicit voltage-gated single-channel currents. The upper trace shows the result in the absence of any blocker, the middle trace is the result in the presence of 19 nM ChTX, and the bottom trace is the result in the presence of 17.5 nM ChTX and 10 mM TEA (with extracellular K^+ reduced to 4.6 mM). The voltage step is at the beginning of each trace. The sampling rate was 2 kHz, and data were filtered at 200 Hz. These data are representative of three such experiments to determine the effect of ChTX on an excised outside-out patch, although this is the only example in which both ChTX and TEA were used simultaneously.

cytes, because it does not exhibit the hypersensitivity to TEA^+ that distinguishes the murine channel (DeCoursey et al., 1987; Lewis and Cahalan, 1988).

DISCUSSION

We were able to distinguish at least three different K^+ channel behaviors in normal, quiescent human peripheral blood T lymphocytes. These currents have different kinetics, voltage sensitivity, and pharmacology; all appeared to have the same unitary conductance of ~10 pS.

Voltage-gated Current

The most prevalent channel was voltage gated and inactivating. Though patches exhibiting activity contained 1.7 channels per patch, it was impossible to know whether patches containing no activity were actually devoid of channels because some

permanent inactivation occurred as a result of patch formation (Lee, S.C., and C. Deutsch, unpublished observations).

Despite the apparent lability of channels in cell-attached recording, the kinetics of the voltage-gated channel were highly consistent among cell-attached patches and did not change appreciably with time of recording. Ensemble averages of the predominant channel showed activation and inactivation that were modeled well with the same Hodgkin-Huxley formulation used to describe the voltage-gated current in whole-cell patch clamp recording (but see below). Although the relative rates of activation and inactivation were essentially the same for both the ensemble and whole-cell currents, the absolute rates were somewhat faster in the single-channel ensemble currents. *A priori* we would have expected the opposite result. In whole-cell configuration, the kinetics of the voltage-gated outward current become faster with time, and the rapidity and extent to which this occurs depends on the major anion in the pipette solution (Cahalan et al., 1985; Deutsch et al., 1986). The rate of inactivation of K^+ channels can be altered by experimental conditions. For example, $I_K(A)$ currents observed in cell-attached patches have faster inactivation rates than the same currents observed in excised inside-out patches (Ruppersberg et al., 1991*b*). Additionally, faster kinetics could be due to a local increase in intracellular Ca^{2+} concentration induced by patch formation, which would lead to an increase in the rate of inactivation of the lymphocyte K^+ channel (Grissmer and Cahalan, 1989), although we would expect such an effect to be transient. Since the kinetics in our recordings are consistent and stable, the faster inactivation kinetics probably reflect the true rate of inactivation in the intact cell.

In a few cases, there was clear evidence of a voltage-gated channel that inactivated three- to fourfold slower than the predominant one. Unitary amplitude and appearance of this conductance were essentially the same as the more quickly inactivating channel. This behavior could indicate the presence of a distinct channel, or it could reflect a variation or modification of one basic type due to endogenous regulators.

The unitary conductance of the voltage-gated channel derived from cell-attached patches was somewhat less than that observed in whole-cell and excised outside-out patches. This was probably due to a reduction in the electrochemical driving force for K^+ due to a voltage shift in whole-cell potential when channels in the patch were open. To observe channels in cell-attached mode at full amplitude, the conductance of the whole-cell membrane must be much greater than that of the cell-attached patch (Fenwick et al., 1982; Fischmeister et al., 1986).

The unitary conductance of the inactivating channel decreased at positive potentials. Deviation from ohmic behavior was not usually seen in whole-cell macroscopic peak current–voltage relations until potentials greater than or equal to +50 mV (Cahalan et al., 1985; Deutsch et al., 1986). This reduction in unitary conductance could reflect the presence of a voltage-sensitive, endogenous modulator, as Na^+ and Mg^{2+} can be for some K^+ channels (Marty, 1983; Matsuda et al., 1987). In lymphocytes we could detect no modulation of whole-cell current with free $[Mg^{2+}]$ up to 2 mM in the pipette; but when we recorded whole-cell current with a pipette solution containing 16 mM Na^+, there was a significant decrease from the expected voltage-gated current at potentials greater than or equal to −10 mV (Lee, S. C., and C. Deutsch, unpublished observations). Since normal $[Na^+]_i$ in T lymphocytes is ~20

mM (Deutsch et al., 1984), Na^+ could be an important modulator of K^+ channel function in the intact cell. The $[Na^+]_i$ in cells bathed in high K^+ may, however, be lower than 20 mM.

Finally, we noted that a Hodgkin-Huxley model gave a good representation of the ensemble and whole-cell currents. However, because there is a 50–100-fold difference between the activation and inactivation time constants, this model would not be very sensitive to deviations from its assumptions. In particular, the Hodgkin-Huxley model assumes that activation and inactivation are independent processes triggered simultaneously by the voltage step and that inactivation proceeds at the same rate from both open and closed states of the channel. Our data are more consistent with a model in which inactivation is coupled to activation and occurs preferentially when the channel is open, as we have argued before on the basis of different data (Lee and Deutsch, 1990). The partially coupled kinetic model developed by Zagotta and Aldrich (1990) to describe the *Shaker* A-type K^+ channel also provides a reasonable description of this lymphocyte K^+ channel. However, in lymphocytes the closed-to-inactivated state transition needed to model the *Shaker* channel is not required. DeCoursey (1990) also reported strong evidence that inactivation can only occur from the open state of a rat alveolar K^+ channel that is very similar to the T cell channel. Moreover, recent molecular biological studies of cloned neuronal $I_K(A)$ channels indicate that inactivation occurs from an open state (Ruppersberg et al., 1991*a*).

Noninactivating Current

The other major type of unitary event observed in cell-attached patches appeared to be both noninactivating and non–voltage gated, and required kinetic parameters different from those of the voltage-gated inactivating channel to describe its behavior. The observed unitary conductance of the noninactivating channel was the same as that of the inactivating channel.

One hypothesis is that this noninactivating channel could be a Ca^{2+}-activated K^+ channel, triggered by a transient increase in intracellular Ca^{2+} concentration (i.e., during patch formation). However, we were unable to demonstrate in experiments with calcium ionophores that the noninactivating channel was Ca^{2+} sensitive. It is possible that Ca^{2+} does not gate this channel, or that other factors might have masked an ionophore-induced response, such as the large Ca^{2+}-buffering capacity of T lymphocytes (Ishida and Chused, 1988), desensitization of the Ca^{2+}-activated channel (Mahaut-Smith and Schlichter, 1989), and/or a very low density of such channels on the T cell surface (Grissmer et al., 1992).

Whole-Cell Current

Long-term depolarization in whole-cell configuration elicited a noninactivating or very slowly inactivating plateau current that was not blocked by ChTX. Single-channel currents observed in whole-cell and excised outside-out patches were not different in amplitude or appearance from the prevalent, inactivating channel, and did not exhibit the characteristic "flickering" behavior of the noninactivating channel observed in cell-attached patches. However, reactivation of the quickly inactivating channel in cell-attached and excised outside-out patches was observed too infre-

quently to account for the magnitude of the plateau current, suggesting that the residual current was produced by a different channel type. Moreover, ChTX experiments such as those shown in Figs. 9 and 11 indicated that a significant fraction of residual channel activity at sustained depolarized voltages was due to a different, ChTX-insensitive channel type. We have not quantified the selectivity of this channel, but the experiments with intracellular Cs^+ and both intracellular and extracellular TEA suggest that most of the residual current was carried by K^+.

The magnitude of the plateau current often decreases with time in whole-cell configuration, especially with high $[F^-]$ in the pipette solution. Difference currents (Fig. 10 *B*) suggest that the component that is lost from the plateau is voltage gated, with threshold near 0 mV, but slowly activating and very slowly inactivating or noninactivating. A slowly rising, noninactivating outward current appearing during voltage steps positive to 0 mV and with apparent reversal around 0 mV has been reported before (Cahalan et al., 1985). Such current could contribute to the time-dependent changes observed typically in the first 10–20 min of whole-cell patch clamp recording in T lymphocytes. These changes include a shift of threshold to more negative voltages and the shortening of activation and inactivation time constants (Cahalan et al., 1985; Deutsch et al., 1986). The threshold shift has been interpreted as deriving from the dissipation of a junction potential, but this shift is insufficient to account for the changes in kinetics. Apparent increase in the rates of activation and inactivation of total current could occur as the slowly activating, noninactivating component disappears. The predominant, inactivating current would remain unchanged, as suggested by the similarity between the kinetic parameters derived from cell-attached and long-term whole-cell recordings. In preliminary experiments using the less invasive whole-cell perforated patch recording technique (Horn and Marty, 1988), we observed plateau current that was typically ~6% of the peak current at +50 mV, and was stable for tens of minutes (Lee, S. C., and C. Deutsch, unpublished observations).

Physiology

We have presented evidence from cell-attached patch recording that there are at least two distinct K^+ channel types in quiescent human T lymphocytes. There are also three other behaviors observed in cell-attached, excised patch or whole-cell recording, including (*a*) slower inactivation, (*b*) noninactivation, and (*c*) ChTX insensitivity, which implicate other channel types and/or modifications of the basic types.

What is the role of each of these channels in T cell function? Thus far, a role for the voltage-gated K^+ channel has been proposed for T lymphocytes in cell volume regulation (Cahalan and Lewis, 1988; Lee et al., 1988; Grinstein and Smith, 1990), mitogen-stimulated proliferation (Chandy et al., 1984; Deutsch et al., 1986; Price et al., 1989), cytotoxic killing (Schlichter et al., 1986), and mitogen-stimulated lymphokine elaboration (Price et al., 1989) and gene expression (Freedman et al., 1991). However, other K^+ channel types or behaviors may also play a role in these cell functions. For example, though ChTX is >1,000-fold more potent than all the non-toxin blockers of the voltage-gated K^+ conductance, it does not fully inhibit and is not as effective as less-specific blockers against either regulatory volume decrease (Grinstein and Smith, 1990) or mitogen-stimulated proliferation (Price et al., 1989),

suggesting that other K^+ pathways are important in these cellular responses. Steady-state levels of activation-associated mRNA, IL-2 elaboration, and proliferation are all influenced by extracellular [K^+] and/or membrane potential (Freedman et al., 1991).

Ca^{2+}-dependent, K^+ blocker–sensitive hyperpolarization is elicited as a result of mitogen addition to T lymphocytes (Tsien et al., 1982; Wilson and Chused, 1985; Lewis and Cahalan, 1989; Grinstein and Smith, 1990), and it has been proposed that this serves to promote the entry of extracellular Ca^{2+} necessary for cell proliferation (Gelfand et al., 1987). Nevertheless, Ca^{2+}-activated K^+ conductance is not correlated with cell proliferation in the same manner as the voltage-gated, inactivating conductance. Inhibition of the Ca^{2+}-induced hyperpolarization by ChTX requires a higher concentration of toxin (Grinstein and Smith, 1990) than that which is effective both to block the voltage-gated channel and to inhibit proliferation (Price et al., 1989).

We have identified at least one type of voltage-gated, ChTX-insensitive but TEA-sensitive K^+ current. This current slowly decreases in whole-cell recording configuration, but may be amenable to further study in perforated patch mode. A K^+ channel with these properties could provide a secondary, Ca^{2+}- and ChTX-insensitive pathway for K^+ movement during volume regulation, as proposed by Grinstein and Smith (1990). Such channel properties may be sufficient to account for the effects of ChTX on proliferation and volume regulation that distinguish this agent from other, less specific blockers of T cell K^+ channels.

In summary, we have characterized a voltage-gated, inactivating K^+ channel on human T lymphocytes that appears to underlie most, but not all, of the whole-cell current. Differences in kinetics between single-channel ensembles and macroscopic currents suggest that subtypes of the basic channel and/or other K^+ channel types contribute to the whole-cell current. Among these are transient, noninactivating channels and ChTX-insensitive channels. All of these channel types are likely to be important in our understanding of human T lymphocyte physiology.

We thank Richard Horn and Pamela Pappone for their critical reading of the manuscript, and Richard Horn for his assistance in analysis of some of the single-channel data.

This work was supported by NIH grant GM-41467 (to C. Deutsch) and the Medical Scientist Training Program 5-T32-GM 07170 (to D. Levy).

Original version received 19 June 1991 and accepted version received 4 February 1992.

REFERENCES

Armstrong, C. M., and F. Bezanilla. 1974. Charge movement associated with the opening and closing of the activation gates of the Na channels. *Journal of General Physiology.* 63:533–552.

Bezanilla, F. 1985. A high capacity data recording device based on a digital audio processor and a video cassette recorder. *Biophysical Journal.* 47:437–441.

Cahalan, M. D., K. G. Chandy, T. E. DeCoursey, and S. Gupta. 1985. A voltage-gated potassium channel in human T lymphocytes. *Journal of Physiology.* 358:197–237.

Cahalan, M. D., and R. S. Lewis. 1988. Role of potassium and chloride channels in volume regulation by T lymphocytes. *In* Cell Physiology of Blood. R. B. Gunn and J. C. Parker, editors. Rockefeller University Press, New York. 281–301.

Chandy, K. G., T. E. DeCoursey, M. D. Cahalan, C. McLaughlin, and S. Gupta. 1984. Voltage-gated

potassium channels are required for T lymphocyte activation. *Journal of Experimental Medicine.* 160:369–385.

DeCoursey, T. E. 1990. State-dependent inactivation of K^+ currents in rat type II alveolar epithelial cells. *Journal of General Physiology.* 95:617–646.

DeCoursey, T. E., K. G. Chandy, S. Gupta, and M. D. Cahalan. 1984. Voltage-dependent K^+ channels in human T lymphocytes: a role in mitogenesis? *Nature.* 307:465–468.

DeCoursey, T. E., K. G. Chandy, S. Gupta, and M. D. Cahalan. 1987. Two types of potassium channels in murine T lymphocytes. *Journal of General Physiology.* 89:379–404.

Deutsch, C., A. Holian, S. K. Holian, R. P. Daniele, and D. F. Wilson. 1979. Transmembrane electrical and pH gradients across human erythrocytes and human peripheral lymphocytes. *Journal of Cellular Physiology.* 98:137–144.

Deutsch, C., D. Krause, and S. C. Lee. 1986. Voltage-gated potassium conductance in human T lymphocytes stimulated with phorbol ester. *Journal of Physiology.* 372:405–423.

Deutsch, C., and S. C. Lee. 1988. Cell volume regulation in lymphocytes. *Renal Physiology and Biochemistry.* 3–5:260–276.

Deutsch, C., and S. C. Lee. 1989. Modulation of K^+ currents in human peripheral blood lymphocytes by pH. *Journal of Physiology.* 413:399–413.

Deutsch, C., M. Price, S. Lee, V. F. King, and M. L. Garcia. 1991. Characterization of high affinity binding sites for charybdotoxin in human T lymphocytes: evidence for association with the voltage-gated K^+ channel. *Journal of Biological Chemistry.* 266:3668–3674.

Deutsch, C., J. S. Taylor, and M. Price. 1984. pH homeostasis in human lymphocytes: modulation by ions and mitogen. *Journal of Cell Biology.* 98:885–893.

Fasolato, C., and T. Pozzan. 1989. Effect of membrane potential on divalent cation transport catalyzed by the "electroneutral" ionophores A23187 and ionomycin. *Journal of Biological Chemistry.* 264:19630–19636.

Fenwick, E. M., A. Marty, and E. Neher. 1982. A patch-clamp study of bovine chromaffin cells and of their sensitivity to acetylcholine. *Journal of Physiology.* 331:577–597.

Fischmeister, R., R. K. Ayer, Jr., and R. L. DeHaan. 1986. Some limitations of the cell-attached patch clamp technique: a two-electrode analysis. *Pflügers Archiv.* 406:73–82.

Freedman, B., M. Price, and C. Deutsch. 1991. Charybdotoxin and high extracellular K^+ specifically decrease IL2 mRNA steady-state levels in stimulated human T lymphocytes. *Biophysical Journal.* 59:453*a*. (Abstr.)

Gallin, E. K. 1991. Ion channels in white blood cells. *Physiological Reviews.* 71:775–811.

Gelfand, E. W., G. B. Mills, R. K. Cheung, J. W. W. Lee, and S. Grinstein. 1987. Transmembrane ion fluxes during activation of human T lymphocytes: role of Ca^{2+}, Na^+/H^+ exchange, and phospholipid turnover. *Immunological Reviews.* 95:60–87.

Grinstein, S., and S. J. Dixon. 1989. Ion transport, membrane potential, and cytoplasmic pH in lymphocytes: changes during activation. *Physiological Reviews.* 69:417–481.

Grinstein, S., and J. D. Smith. 1990. Calcium-independent cell volume regulation in human lymphocytes. Inhibition by charybdotoxin. *Journal of General Physiology.* 95:97–120.

Grissmer, S., and M. D. Cahalan. 1989. Divalent ion trapping inside potassium channels of human T lymphocytes. *Journal of General Physiology.* 93:609–639.

Grissmer, S., and M. D. Cahalan. 1991. Ca^{2+}-activated K^+ channels in resting and activated human peripheral T lymphocytes. *Biophysical Journal.* 59:213*a*. (Abstr.)

Grissmer, S., A. N. Nguyen, and M. D. Cahalan. 1992. Characterization of Ca^2-activated K^+ channels in resting and activated human peripheral T lymphocytes. *Biophysical Journal.* 61:A14. (Abstr.)

Hamill, O. P., A. Marty, E. Neher, B. Sakmann, and F. J. Sigworth. 1981. Improved patch-clamp techniques for high-resolution current recording from cells and cell-free membrane patches. *Pflügers Archiv.* 391:85–100.

Hodgkin, A. L., and A. F. Huxley. 1952. A quantitative description of membrane current and its application to conduction and excitation in nerve. *Journal of Physiology.* 117:500–544.

Horn, R., and A. Marty. 1988. Muscarinic activation of ionic currents measured by a new whole-cell recording method. *Journal of General Physiology.* 92:145–159.

Ishida, Y., and T. M. Chused. 1988. Heterogeneity of lymphocyte calcium metabolism is caused by T cell-specific calcium-sensitive potassium channel and sensitivity of the calcium ATPase pump to membrane potential. *Journal of Experimental Medicine.* 168:839–852.

Lee, S. C., and C. Deutsch. 1990. Temperature dependence of K^+-channel properties in human T lymphocytes. *Biophysical Journal.* 57:49–62.

Lee, S. C., D. Levy, and C. Deutsch. 1991. Single channel K^+ currents in primary human T lymphocytes. *Biophysical Journal.* 59:453*a*. (Abstr.)

Lee, S. C., M. Price, M. B. Prystowsky, and C. Deutsch. 1988. Volume response of quiescent and interleukin 2-stimulated T-lymphocytes to hypotonicity. *American Journal of Physiology.* 254:C286–C296.

Lewis, R. S., and M. D. Cahalan. 1988. Subset-specific expression of potassium channels in developing murine T lymphocytes. *Science.* 239:771–775.

Lewis, R. S., and M. D. Cahalan. 1989. Mitogen-induced oscillations of cytosolic Ca^{2+} and transmembrane Ca^{2+} current in human leukemic T cells. *Cell Regulation.* 1:99–112.

Lewis, R. S., and M. D. Cahalan. 1990. Ion channels and signal transduction in lymphocytes. *Annual Review of Physiology.* 52:415–430.

Mahaut-Smith, M. P., and L. C. Schlichter. 1989. Ca^{2+}-activated K^+ channels in human B lymphocytes and rat thymocytes. *Journal of Physiology.* 415:69–83.

Marty, A. 1983. Blocking of large unitary calcium-dependent potassium currents by internal sodium ions. *Pflügers Archiv.* 396:179–181.

Matsuda, H., A. Saigusa, and H. Irisawa. 1987. Ohmic conductance through the inwardly rectifying K channel and blocking by internal Mg^{2+}. *Nature.* 325:156–159.

Matteson, D. R., and C. Deutsch. 1984. K channels in T lymphocytes: a patch-clamp study using monoclonal antibody adhesion. *Nature.* 307:468–471.

Patlak, J., and R. Horn. 1982. Effect of N-bromoacetamide on single sodium channel currents in excised membrane patches. *Journal of General Physiology.* 79:333–351.

Price, M., S. C. Lee, and C. Deutsch. 1989. Charybdotoxin inhibits proliferation and interleukin 2 production in human peripheral blood lymphocytes. *Proceedings of the National Academy of Sciences, USA.* 86:10171–10175.

Ruppersberg, J. P., R. Frank, O. Pongs, and M. Stocker. 1991*a*. Cloned neuronal $I_K(A)$ channels reopen during recovery from inactivation. *Nature.* 353:657–660.

Ruppersberg, J. P., M. Stocker, O. Pongs, S. H. Heinemann, R. Frank, and M. Koenen. 1991*b*. Regulation of fast inactivation of cloned mammalian $I_K(A)$ channels by cysteine oxidation. *Nature.* 352:711–714.

Sands, S. B., R. S. Lewis, and M. D. Cahalan. 1989. Charybdotoxin blocks voltage-gated K^+ channels in human and murine T lymphocytes. *Journal of General Physiology.* 93:1061–1074.

Schlichter, L., N. Sidell, and S. Hagiwara. 1986. Potassium channels mediate killing by human natural killer cells. *Proceedings of the National Academy of Sciences, USA.* 83:451–455.

Tsien, R. Y., T. Pozzan, and T. J. Rink. 1982. T-cell mitogens cause early changes in cytoplasmic free Ca^{2+} and membrane potential in lymphocytes. *Nature.* 295:68–70.

Wilson, H. A., and T. M. Chused. 1985. Lymphocyte membrane potential and Ca^{2+}-sensitive potassium channels described by oxonol dye fluorescence measurements. *Journal of Cellular Physiology.* 125:72–81.

Zagotta, W. N., and R. W. Aldrich. 1990. Voltage-dependent gating of *Shaker* A-type potassium channels in *Drosophila* muscle. *Journal of General Physiology.* 95:29–60.